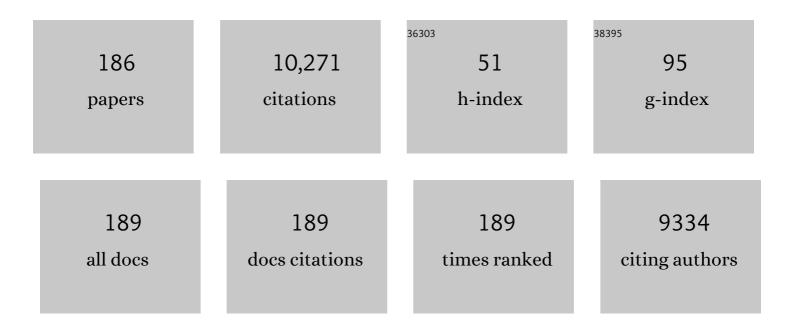
Yiping Guo

List of Publications by Year in descending order

Source: https://exaly.com/author-pdf/880444/publications.pdf Version: 2024-02-01



YIDING GUO

#	Article	IF	CITATIONS
1	Phase transitional behavior and piezoelectric properties of (Na0.5K0.5)NbO3–LiNbO3 ceramics. Applied Physics Letters, 2004, 85, 4121-4123.	3.3	1,394
2	(Na0.5K0.5)NbO3–LiTaO3 lead-free piezoelectric ceramics. Materials Letters, 2005, 59, 241-244.	2.6	582
3	Effects of carbon nanotube functionalization on the mechanical and thermal properties of epoxy composites. Carbon, 2009, 47, 1723-1737.	10.3	381
4	Dielectric and piezoelectric properties of lead-free (Na0.5K0.5)NbO3–SrTiO3 ceramics. Solid State Communications, 2004, 129, 279-284.	1.9	349
5	Raman Scattering Study of Piezoelectric (Na0.5K0.5)NbO3-LiNbO3Ceramics. Japanese Journal of Applied Physics, 2005, 44, 7064-7067.	1.5	306
6	Characterization and dielectric behavior of willemite and TiO2-doped willemite ceramics at millimeter-wave frequency. Journal of the European Ceramic Society, 2006, 26, 1827-1830.	5.7	239
7	Structure and Electrical Properties of Lead-Free (Na0.5K0.5)NbO3-BaTiO3Ceramics. Japanese Journal of Applied Physics, 2004, 43, 6662-6666.	1.5	231
8	lonic Conductivity and Air Stability of Al-Doped Li ₇ La ₃ Zr ₂ O ₁₂ Sintered in Alumina and Pt Crucibles. ACS Applied Materials & Interfaces, 2016, 8, 5335-5342.	8.0	229
9	Fabrication of ultralight three-dimensional graphene networks with strong electromagnetic wave absorption properties. Journal of Materials Chemistry A, 2015, 3, 3739-3747.	10.3	219
10	Large Electric Field-Induced Strain and Antiferroelectric Behavior in (1- <i>x</i>)(Na _{0.5} Bi _{0.5})TiO ₃ - <i>x</i> BaTiO ₃ Ceramics. Chemistry of Materials, 2011, 23, 219-228.	6.7	178
11	Reaction mechanisms of lithium garnet pellets in ambient air: The effect of humidity and CO ₂ . Journal of the American Ceramic Society, 2017, 100, 2832-2839.	3.8	167
12	Dielectric and piezoelectric performance of PMN–PT single crystals with compositions around the MPB: influence of composition, poling field and crystal orientation. Materials Science and Engineering B: Solid-State Materials for Advanced Technology, 2002, 96, 254-262.	3.5	154
13	Li 3 PO 4 -added garnet-type Li 6.5 La 3 Zr 1.5 Ta 0.5 O 12 for Li-dendrite suppression. Journal of Power Sources, 2017, 354, 68-73.	7.8	150
14	Sizing of Rainwater Storage Units for Green Building Applications. Journal of Hydrologic Engineering - ASCE, 2007, 12, 197-205.	1.9	140
15	xmins:mml="http://www.w3.org/1998/Math/Math/MathML" display="inline"> <mml:mrow><mml:mo stretchy="false">(<mml:msub><mml:mi) (matl<="" 0.784314="" 1="" 10="" 187="" 50="" etqq1="" overlock="" rgbt="" td="" tf="" tj=""><td>nvariant=" 3.2</td><td>normal">Na< 135</td></mml:mi)></mml:msub></mml:mo </mml:mrow>	nvariant=" 3.2	normal">Na< 135
16	The phase transition sequence and the location of the morphotropic phase boundary region in (1 Â) Tj ETQq0 0 (D rgBT /Ov	erlock 10 Tf
17	Facile synthesis of V ⁴⁺ self-doped, [010] oriented BiVO ₄ nanorods with highly efficient visible light-induced photocatalytic activity. Physical Chemistry Chemical Physics, 2014, 16, 24519-24526.	2.8	134

¹⁸Hydrologic analysis of urban catchments with event-based probabilistic models: 1. Runoff volume.4.211818Water Resources Research, 1998, 34, 3421-3431.4.2118

#	Article	IF	CITATIONS
19	The effect of annealing on a 3D SnO2/graphene foam as an advanced lithium-ion battery anode. Scientific Reports, 2016, 6, 19195.	3.3	112
20	Evidence for oxygen vacancy or ferroelectric polarization induced switchable diode and photovoltaic effects in BiFeO ₃ based thin films. Nanotechnology, 2013, 24, 275201.	2.6	110
21	Synthesis of Orthorhombic Perovskite-Type ZnSnO ₃ Single-Crystal Nanoplates and Their Application in Energy Harvesting. ACS Applied Materials & Interfaces, 2017, 9, 8271-8279.	8.0	105
22	Design for Highly Piezoelectric and Visible/Nearâ€Infrared Photoresponsive Perovskite Oxides. Advanced Materials, 2019, 31, e1805802.	21.0	101
23	Effect of composition and poling field on the properties and ferroelectric phase-stability of Pb(Mg1/3Nb2/3)O3–PbTiO3 crystals. Journal of Applied Physics, 2002, 92, 6134-6138.	2.5	99
24	Selfâ€Healing Shape Memory PUPCL Copolymer with High Cycle Life. Advanced Functional Materials, 2018, 28, 1704109.	14.9	87
25	Electro-active shape memory composites enhanced by flexible carbon nanotube/graphene aerogels. Journal of Materials Chemistry A, 2015, 3, 11641-11649.	10.3	85
26	Dielectric and piezoelectric properties of highly (100)-oriented BaTiO3 thin film grown on a Pt/TiOx/SiO2/Si substrate using LaNiO3 as a buffer layer. Journal of Crystal Growth, 2005, 284, 190-196.	1.5	84
27	Ferroelectric-relaxor behavior of (Na0.5K0.5)NbO3-based ceramics. Journal of Physics and Chemistry of Solids, 2004, 65, 1831-1835.	4.0	82
28	Enhanced Photovoltaic Performance of Perovskite Solar Cells Using Polymer P(VDF-TrFE) as a Processed Additive. Journal of Physical Chemistry C, 2016, 120, 12980-12988.	3.1	81
29	Hydrologic Design of Urban Flood Control Detention Ponds. Journal of Hydrologic Engineering - ASCE, 2001, 6, 472-479.	1.9	77
30	Giant Magnetodielectric Effect in 0â^'3 Ni _{0.5} Zn _{0.5} Fe ₂ O ₄ -Poly(vinylidene-fluoride) Nanocomposite Films. Journal of Physical Chemistry C, 2010, 114, 13861-13866.	3.1	77
31	Growth and piezoelectric properties of Pb(Mg1/3Nb2/3)O3–PbTiO3 crystals by the modified Bridgman technique. Solid State Communications, 2001, 120, 321-324.	1.9	76
32	In situ preparation of carbon/Fe 3 C composite nanofibers with excellent electromagnetic wave absorption properties. Composites Part A: Applied Science and Manufacturing, 2017, 92, 33-41.	7.6	75
33	Analytical Probabilistic Model for Evaluating the Hydrologic Performance of Green Roofs. Journal of Hydrologic Engineering - ASCE, 2013, 18, 19-28.	1.9	72
34	CoSe/Co nanoparticles wrapped by in situ grown N-doped graphitic carbon nanosheets as anode material for advanced lithium ion batteries. Journal of Power Sources, 2018, 399, 223-230.	7.8	70
35	MOF-Derived Hollow Co ₃ S ₄ Quasi-polyhedron/MWCNT Nanocomposites as Electrodes for Advanced Lithium Ion Batteries and Supercapacitors. ACS Applied Energy Materials, 2018, 1, 402-410.	5.1	69
36	Multistep sintering to synthesize fast lithium garnets. Journal of Power Sources, 2016, 302, 291-297.	7.8	68

#	Article	IF	CITATIONS
37	Peculiar properties of a high Curie temperature Pb(In1/2Nb1/2)O3–PbTiO3 single crystal grown by the modified Bridgman technique. Solid State Communications, 2002, 123, 417-420.	1.9	67
38	Dielectric and ferroelectric properties of highly (100)-oriented (Na0.5Bi0.5)0.94Ba0.06TiO3 thin films grown on LaNiO3/γ-Al2O3/Si substrates by chemical solution deposition. Solid State Sciences, 2008, 10, 928-933.	3.2	66
39	Synthesis of hierarchical TS-1 zeolite via a novel three-step crystallization method and its excellent catalytic performance in oxidative desulfurization. Fuel, 2017, 188, 232-238.	6.4	65
40	An analytical probabilistic approach to sizing flood control detention facilities. Water Resources Research, 1999, 35, 2457-2468.	4.2	62
41	Updating Rainfall IDF Relationships to Maintain Urban Drainage Design Standards. Journal of Hydrologic Engineering - ASCE, 2006, 11, 506-509.	1.9	61
42	Enhanced Photovoltaic Effect in BiVO ₄ Semiconductor by Incorporation with an Ultrathin BiFeO ₃ Ferroelectric Layer. ACS Applied Materials & Interfaces, 2013, 5, 6925-6929.	8.0	60
43	Hydrologic analysis of urban catchments with event-based probabilistic models: 2. Peak discharge rate. Water Resources Research, 1998, 34, 3433-3443.	4.2	58
44	Facile synthesis of hierarchical TS-1 zeolite without using mesopore templates and its application in deep oxidative desulfurization. Microporous and Mesoporous Materials, 2019, 275, 61-68.	4.4	58
45	Superflexible and Lead-Free Piezoelectric Nanogenerator as a Highly Sensitive Self-Powered Sensor for Human Motion Monitoring. Nano-Micro Letters, 2021, 13, 117.	27.0	57
46	Uncertainty of nitrate-N load computations for agricultural watersheds. Water Resources Research, 2002, 38, 3-1-3-12.	4.2	56
47	Dependence of high electric-field-induced strain on the composition and orientation of Pb(Mg1/3Nb2/3)O3–PbTiO3 crystals. Solid State Communications, 2003, 126, 347-351.	1.9	56
48	Highly-efficient piezocatalytic performance of nanocrystalline BaTi0.89Sn0.11O3 catalyst with Tc near room temperature. Nano Energy, 2021, 85, 106028.	16.0	56
49	Enhanced photovoltaic properties in polycrystalline BiFeO3 thin films with rhombohedral perovskite structure deposited on fluorine doped tin oxide substrates. Materials Letters, 2012, 88, 140-142.	2.6	55
50	Piezoelectric thin film on glass fiber fabric with structural hierarchy: An approach to high-performance, superflexible, cost-effective, and large-scale nanogenerators. Nano Energy, 2019, 59, 745-753.	16.0	54
51	Visible or Near-Infrared Light Self-Powered Photodetectors Based on Transparent Ferroelectric Ceramics. ACS Applied Materials & Interfaces, 2020, 12, 33950-33959.	8.0	54
52	Photovoltaic properties of BiFeO3 thin film capacitors by using Al-doped zinc oxide as top electrode. Materials Letters, 2013, 91, 359-361.	2.6	53
53	Stormwater Capture Efficiency of Bioretention Systems. Water Resources Management, 2014, 28, 149-168.	3.9	53
54	Contaminant occurrence and migration between high- and low-permeability zones in groundwater systems: A review. Science of the Total Environment, 2020, 743, 140703.	8.0	53

#	Article	IF	CITATIONS
55	SWMM Simulation of the Storm Water Volume Control Performance of Permeable Pavement Systems. Journal of Hydrologic Engineering - ASCE, 2015, 20, .	1.9	52
56	Antiferroelectric Phase and Pyroelectric Response in (NayBiz)Ti1â^'xO3(1â^'x)-xBaTiO3 Ceramics. Journal of the American Ceramic Society, 2011, 94, 1350-1353.	3.8	49
57	Three dimensional Graphene aerogels as binder-less, freestanding, elastic and high-performance electrodes for lithium-ion batteries. Scientific Reports, 2016, 6, 27365.	3.3	49
58	3D composites of layered MoS ₂ and graphene nanoribbons for high performance lithium-ion battery anodes. Journal of Materials Chemistry A, 2016, 4, 13148-13154.	10.3	47
59	Engineering the Defects and Microstructures in Ferroelectrics for Enhanced/Novel Properties: An Emerging Way to Cope with Energy Crisis and Environmental Pollution. Advanced Science, 2022, 9, e2105368.	11.2	46
60	A facile method to fabricate polyurethane based graphene foams/epoxy/carbon nanotubes composite for electro-active shape memory application. Composites Part A: Applied Science and Manufacturing, 2016, 91, 292-300.	7.6	43
61	Dielectric Modulated Glass Fiber Fabricâ€Based Single Electrode Triboelectric Nanogenerator for Efficient Biomechanical Energy Harvesting. Advanced Functional Materials, 2021, 31, 2102431.	14.9	43
62	Explicit Equation for Estimating Storm-Water Capture Efficiency of Rain Gardens. Journal of Hydrologic Engineering - ASCE, 2013, 18, 1739-1748.	1.9	41
63	Domain Configuration and Ferroelectric Related Properties of the (110)cubCuts of Relaxor-Based Pb(Mg1/3Nb2/3)O3–PbTiO3Single Crystals. Japanese Journal of Applied Physics, 2002, 41, 1451-1454.	1.5	40
64	Trap-State Passivation by Nonvolatile Small Molecules with Carboxylic Acid Groups for Efficient Planar Perovskite Solar Cells. Journal of Physical Chemistry C, 2019, 123, 14223-14228.	3.1	40
65	Threshold analysis of rainstorm depth and duration statistics at Toronto, Canada. Journal of Hydrology, 2008, 348, 535-545.	5.4	39
66	Ferroelectric and pyroelectric properties of (Na0.5Bi0.5)TiO3–BaTiO3 based trilayered thin films. Thin Solid Films, 2009, 517, 2974-2978.	1.8	39
67	Probabilistic rainfallâ€runoff transformation considering both infiltration and saturation excess runoff generation processes. Water Resources Research, 2012, 48, .	4.2	38
68	Cholecystokinin release triggered by NMDA receptors produces LTP and sound–sound associative memory. Proceedings of the National Academy of Sciences of the United States of America, 2019, 116, 6397-6406.	7.1	38
69	Urban flood risk assessment using storm characteristic parameters sensitive to catchment-specific drainage system. Science of the Total Environment, 2019, 659, 1362-1369.	8.0	37
70	Lead-free BiFeO3 film on glass fiber fabric: Wearable hybrid piezoelectric-triboelectric nanogenerator. Ceramics International, 2021, 47, 3573-3579.	4.8	37
71	Growth and electrical properties of Pb(Sc1/2Nb1/2)O3–Pb(Mg1/3Nb2/3)O3–PbTiO3 ternary single crystals by a modified Bridgman technique. Journal of Crystal Growth, 2001, 226, 111-116.	1.5	35
72	Enhanced Photovoltaic Performance in Polycrystalline BiFeO ₃ Thin Film/ZnO Nanorod Heterojunctions. Journal of Physical Chemistry C, 2014, 118, 15200-15206.	3.1	35

#	Article	IF	CITATIONS
73	Facile preparation of highly cost-effective BaSO4@BiVO4 core-shell structured brilliant yellow pigment. Dyes and Pigments, 2016, 128, 49-53.	3.7	34
74	In situ preparation of flower-like α-Ni(OH)2 and NiO from nickel formate with excellent capacitive properties as electrode materials for supercapacitors. Materials Chemistry and Physics, 2015, 151, 160-166.	4.0	33
75	Stochastic modelling of the hydrologic operation of rainwater harvesting systems. Journal of Hydrology, 2018, 562, 30-39.	5.4	33
76	Analysis of detention ponds for storm water quality control. Water Resources Research, 1999, 35, 2447-2456.	4.2	32
77	Ternary oxide BaSnO3 nanoparticles as an efficient electron-transporting layer for planar perovskite solar cells. Journal of Alloys and Compounds, 2017, 722, 196-206.	5.5	32
78	Synthesis of hierarchically porous TS-1 zeolite with excellent deep desulfurization performance under mild conditions. Microporous and Mesoporous Materials, 2018, 264, 272-280.	4.4	32
79	Synthesis and properties of ZnFe 2 O 4 replica with biological hierarchical structure. Materials Science and Engineering B: Solid-State Materials for Advanced Technology, 2013, 178, 1057-1061.	3.5	31
80	Highâ€Coulombicâ€Efficiency Carbon/Li Clusters Composite Anode without Precycling or Prelithiation. Small, 2018, 14, e1802226.	10.0	31
81	Electric-field-induced strain and piezoelectric properties of a high Curie temperature Pb(In1/2Nb1/2)O3–PbTiO3 single crystal. Materials Research Bulletin, 2003, 38, 857-864.	5.2	30
82	BiFeO3–(Na0.5Bi0.5)TiO3 butterfly wing scales: Synthesis, visible-light photocatalytic and magnetic properties. Journal of the European Ceramic Society, 2012, 32, 4335-4340.	5.7	30
83	Electrical properties of (100)-predominant BaTiO3 films derived from alkoxide solutions of two concentrations. Acta Materialia, 2006, 54, 3893-3898.	7.9	29
84	Photoelectrochemical response and electronic structure analysis of mono-dispersed cuboid-shaped Bi ₂ Fe ₄ O ₉ crystals with near-infrared absorption. RSC Advances, 2014, 4, 28209-28218.	3.6	29
85	Boosting piezoelectric response of KNNâ€based ceramics with strong visibleâ€light absorption. Journal of the American Ceramic Society, 2019, 102, 6422-6426.	3.8	29
86	Runoff Reduction Capabilities and Irrigation Requirements of Green Roofs. Water Resources Management, 2014, 28, 1363-1378.	3.9	28
87	Phase transition and piezoelectric properties of dense (K0.48,Na0.52)0.95Li0.05Sb Nb()O3-0.03Ca0.5(Bi0.5,Na0.5)0.5ZrO3 lead free ceramics. Journal of Alloys and Compounds, 2016, 664, 503-509.	5.5	28
88	Structure and electrical properties of trilayered BaTiO3/(Na0.5Bi0.5)TiO3–BaTiO3/BaTiO3 thin films deposited on Si substrate. Solid State Communications, 2009, 149, 14-17.	1.9	27
89	Visible/near-infrared light absorbed nano-ferroelectric for efficient photo-piezocatalytic water splitting and pollutants degradation. Journal of Hazardous Materials, 2021, 416, 125808.	12.4	27
90	Continuously enhanced photoactivity of hierarchical β-Bi2O3/Bi2S3 heterostructure derived from novel BiO2CH3 octagonal nanoplates. Applied Catalysis A: General, 2016, 514, 146-153.	4.3	26

#	Article	IF	CITATIONS
91	Fabricating fast triggered electro-active shape memory graphite/silver nanowires/epoxy resin composite from polymer template. Scientific Reports, 2017, 7, 5535.	3.3	26
92	Zn2SnO4-carbon cloth freestanding flexible anodes for high-performance lithium-ion batteries. Materials and Design, 2018, 156, 272-277.	7.0	26
93	Boosting the Photocatalytic Ability of Bandgap Engineered (Na _{0.5} Bi _{0.5})TiO ₃ –BaTiO ₃ by N–Ni Codoping. Journal of Physical Chemistry C, 2020, 124, 11810-11818.	3.1	26
94	Stretchable, strong and self-healing hydrogel by oxidized CNT-polymer composite. Composites Part A: Applied Science and Manufacturing, 2016, 90, 250-260.	7.6	25
95	An Analytical Stochastic Approach for Evaluating the Performance of Combined Sewer Overflow Tanks. Water Resources Research, 2018, 54, 3357-3375.	4.2	25
96	Response of intergrown microstructure to an electric field and its consequences in the lead-free piezoelectric bismuth sodium titanate. Journal of Solid State Chemistry, 2012, 187, 309-315.	2.9	24
97	Encoding and Retrieval of Artificial Visuoauditory Memory Traces in the Auditory Cortex Requires the Entorhinal Cortex. Journal of Neuroscience, 2013, 33, 9963-9974.	3.6	24
98	Exponentiality Test Procedures for Large Samples of Rainfall Event Characteristics. Journal of Hydrologic Engineering - ASCE, 2016, 21, .	1.9	24
99	Ferroelectric and pyroelectric properties of highly (110)-oriented Pb(Zr0.40Ti0.60)O3 thin films grown on Ptâ^•LaNiO3â^•SiO2â^•Si substrates. Applied Physics Letters, 2007, 90, 232908.	3.3	23
100	Facile preparation of hierarchical titanium silicalite-1 (TS-1) with efficient oxidation of cyclic alkenes using PVA modified MWCNTs as templates. Journal of Alloys and Compounds, 2017, 699, 386-391.	5.5	23
101	Hierarchically designed nanocomposites for triboelectric nanogenerator toward biomechanical energy harvester and smart home system. Nano Energy, 2022, 95, 107047.	16.0	23
102	Analytical probabilistic flood routing for urban stormwater management purposes. Canadian Journal of Civil Engineering, 2008, 35, 487-499.	1.3	21
103	A correlated electron diffraction, <i>in situ</i> neutron diffraction and dielectric properties investigation of poled (1- <i>x</i>)Bi0.5Na0.5TiO3- <i>x</i> BaTiO3 ceramics. Journal of Applied Physics, 2011, 110, .	2.5	21
104	Peak Discharge Estimation Using Analytical Probabilistic and Design Storm Approaches. Journal of Hydrologic Engineering - ASCE, 2006, 11, 46-54.	1.9	20
105	A probabilistic description of rain storms incorporating peak intensities. Journal of Hydrology, 2011, 409, 71-80.	5.4	20
106	A green method to prepare TiO ₂ /MWCNT nanocomposites with high photocatalytic activity and insights into the effect of heat treatment on photocatalytic activity. RSC Advances, 2015, 5, 13430-13436.	3.6	20
107	Analytical Equation for Estimating the Stormwater Capture Efficiency of Permeable Pavement Systems. Journal of Irrigation and Drainage Engineering - ASCE, 2015, 141, .	1.0	20
108	Stochastic Analysis of Hydrologic Operation of Green Roofs. Journal of Hydrologic Engineering - ASCE, 2016, 21, .	1.9	20

#	Article	IF	CITATIONS
109	Facile preparation of high-quality perovskites for efficient solar cells via a fast conversion of wet Pbl ₂ precursor films. RSC Advances, 2017, 7, 22492-22500.	3.6	20
110	Oriented growth of Li metal for stable Li/carbon composite negative electrode. Electrochimica Acta, 2018, 292, 227-233.	5.2	20
111	Understanding the Role of Oxygen Vacancy in Visible–Nearâ€Infraredâ€Lightâ€Absorbing Ferroelectric Perovskite Oxides Created by Offâ€Stoichiometry. Advanced Electronic Materials, 2019, 5, 1900407.	5.1	20
112	Analyzing the Impact of Impervious Area Disconnection on Urban Runoff Control Using an Analytical Probabilistic Model. Water Resources Management, 2019, 33, 1753-1768.	3.9	20
113	Dielectric and optical properties of BiFeO3–(Na0.5Bi0.5)TiO3 thin films deposited on Si substrate using LaNiO3 as buffer layer for photovoltaic devices. Journal of Alloys and Compounds, 2012, 513, 154-158.	5.5	19
114	Synthesis and visible-light photocatalysis capability of BiFeO3–(Na0.5Bi0.5)TiO3 nanopowders by a sol–gel method. Solid State Sciences, 2013, 19, 69-72.	3.2	19
115	Stochastic analysis of storm water quality control detention ponds. Journal of Hydrology, 2019, 571, 573-584.	5.4	19
116	Photoelectric properties of BiVO4 thin films deposited on fluorine doped tin oxide substrates by a modified chemical solution deposition process. International Journal of Hydrogen Energy, 2014, 39, 5569-5574.	7.1	18
117	Enhanced hole transport in benzoic acid doped spiro-OMeTAD composite layer with intergrowing benzoate phase for perovskite solar cells. Journal of Alloys and Compounds, 2020, 832, 154991.	5.5	18
118	Enhanced Visible Photocatalytic Hydrogen Evolution of KN-Based Semiconducting Ferroelectrics <i>via</i> Band-Gap Engineering and High-Field Poling. ACS Applied Materials & Interfaces, 2022, 14, 8916-8930.	8.0	18
119	Thickness Dependence of Electrical Properties of Highly (100)-Oriented BaTiO3Thin Films Prepared by One-Step Chemical Solution Deposition. Japanese Journal of Applied Physics, 2006, 45, 855-859.	1.5	17
120	5-HT2 receptors mediate functional modulation of GABAa receptors and inhibitory synaptic transmissions in human iPS-derived neurons. Scientific Reports, 2016, 6, 20033.	3.3	17
121	Analytical Equations for Estimating the Total Runoff Reduction Efficiency of Infiltration Trenches. Journal of Sustainable Water in the Built Environment, 2016, 2, .	1.6	17
122	Stormwater capture and antecedent moisture characteristics of permeable pavements. Hydrological Processes, 2018, 32, 2708-2720.	2.6	17
123	Reprogramming somatic cells to cells with neuronal characteristics by defined medium both in vitro and in vivo. Cell Regeneration, 2015, 4, 4:12.	2.6	16
124	Composition induced rhombohedral–tetragonal phase boundary and high piezoelectric activity in (K) Tj ETQc Solid State Communications, 2017, 259, 29-33.	0 0 0 rgBT 1.9	/Overlock 10 16
125	Streamflow Forecast Errors and Their Impacts on Forecast-based Reservoir Flood Control. Water Resources Management, 2015, 29, 4557-4572.	3.9	15
126	Intrinsic relationship between energy consumption, pressure, and leakage in water distribution systems. Urban Water Journal, 2017, 14, 515-521.	2.1	15

#	Article	IF	CITATIONS
127	Achieving Ultrahigh Photocurrent Density of Mg/Mn-Modified KNbO ₃ Ferroelectric Semiconductors by Bandgap Engineering and Polarization Maintenance. Chemistry of Materials, 2022, 34, 4274-4285.	6.7	15
128	Dielectric and tunable properties of highly (110)-oriented (Ba0.65Sr0.35)TiO3 thin films deposited on Pt/LaNiO3/SiO2/Si substrates. Journal of Sol-Gel Science and Technology, 2009, 49, 66-70.	2.4	14
129	Analytical Probabilistic Approach for Estimating Design Flood Peaks of Small Watersheds. Journal of Hydrologic Engineering - ASCE, 2011, 16, 847-857.	1.9	14
130	Solvent-assisted growth of organic–inorganic hybrid perovskites with enhanced photovoltaic performances. Solar Energy Materials and Solar Cells, 2015, 143, 360-368.	6.2	14
131	Visuoauditory Associative Memory Established with Cholecystokinin Under Anesthesia Is Retrieved in Behavioral Contexts. Journal of Neuroscience, 2020, 40, 2025-2037.	3.6	14
132	Excellent thermal stability and enhanced piezoelectric performance of Bi(Ni _{2/3} Nb _{1/3})O ₃ â€modified BiFeO ₃ –BaTiO ₃ ceramics. Journal of the American Ceramic Society, 2022, 105, 317-326.	3.8	14
133	Climate Model Simulation of Point Rainfall Frequency Characteristics. Journal of Hydrologic Engineering - ASCE, 2006, 11, 547-554.	1.9	13
134	L-Moment-Based Regional Frequency Analysis of Annual Extreme Precipitation and its Uncertainty Analysis. Water Resources Management, 2017, 31, 3899-3919.	3.9	13
135	Photovoltaic effect of a bilayer thin film with (Na _{0.5} Bi _{0.5} O.5) _{1â^²<i>x</i>} Ba _{<i>x</i>} TiO ₃ /BiFeO< Journal Physics D: Applied Physics, 2013, 46, 365304.	spabas>3 <td>ub2heteros</td>	u b2 heteros
136	Oxygen vacancies induced self-assembling synthesis of V 4+ -BiVO 4 /rGO core-shell nanorods with enhanced water splitting efficiency and superior sewage purification capability. Applied Catalysis A: General, 2016, 526, 105-112.	4.3	12
137	3D composites of ZnSnO3 nanoplates/reduced graphene oxide aerogels as an advanced lithium-ion battery anode. Journal of Materials Science: Materials in Electronics, 2018, 29, 5299-5306.	2.2	12
138	Field-Induced Orthorhombic Phase in Relaxor-Based Ferroelectric Single Crystals Pb(Mg 1/3 Nb 2/3)O 3 -PbTiO 3. Ferroelectrics, 2002, 281, 79-86.	0.6	11
139	Expanded analytical probabilistic stormwater models for use in watershed and master drainage planning. Canadian Journal of Civil Engineering, 2009, 36, 933-943.	1.3	11
140	Morphology of nanotube arrays grown on Ti–35Nb–2Ta–3Zr alloys with different deformations. Applied Surface Science, 2014, 290, 308-312.	6.1	11
141	Derived flood frequency distributions considering individual event hydrograph shapes. Journal of Hydrology, 2017, 547, 296-308.	5.4	11
142	Dynamic water balance of infiltration-based stormwater best management practices. Journal of Hydrology, 2020, 589, 125174.	5.4	11
143	Phase structure, microstructure, and piezoelectric properties of potassium-sodium niobate-based lead-free ceramics modified by Ca. Journal of Alloys and Compounds, 2017, 693, 950-954.	5.5	10
144	Copula-Based Analysis of Flood Peak Level and Duration: Two Case Studies in Taihu Basin, China. Journal of Hydrologic Engineering - ASCE, 2018, 23, .	1.9	10

#	Article	IF	CITATIONS
145	Optical properties of BiFeO3–(Na0.5Bi0.5)TiO3 thin films deposited on glass substrates by chemical solution deposition. Materials Letters, 2012, 71, 60-62.	2.6	9
146	Analytical Equations for Use in the Planning of Infiltration Facilities. Journal of Sustainable Water in the Built Environment, 2018, 4, .	1.6	9
147	Three dimensional nylon66@carbon nanotube aerogel: A platform for high-performance electromagnetic wave absorbing composites. Materials Letters, 2019, 247, 147-150.	2.6	9
148	Retrograde monosynaptic tracing through an engineered human embryonic stem cell line reveals synaptic inputs from host neurons to grafted cells. Cell Regeneration, 2019, 8, 1-8.	2.6	9
149	Piezoelectric Nanogenerators Based on Self-Poled Two-Dimensional Li-Doped ZnO Microdisks. Journal of Electronic Materials, 2019, 48, 2886-2894.	2.2	9
150	The performance of Pt bottom electrode and PZT films deposited on Al2O3 /Si substrate by using LaNiO3 film as an adhesion layer. Solid State Communications, 2008, 145, 413-417.	1.9	8
151	Derived Flow–Duration Relationships for Surface Runoff Dominated Small Urban Streams. Journal of Hydrologic Engineering - ASCE, 2009, 14, 42-52.	1.9	8
152	Probabilistic approach to estimating the effects of channel reaches on flood frequencies. Water Resources Research, 2009, 45, .	4.2	8
153	Improved dielectric stability of epoxy composites with ultralow boron nitride loading. RSC Advances, 2019, 9, 4344-4350.	3.6	8
154	Effects of EDTA on adsorption of Cd(II) and Pb(II) by soil minerals in low-permeability layers: batch experiments and microscopic characterization. Environmental Science and Pollution Research, 2020, 27, 41623-41638.	5.3	8
155	Proper Sizing of Infiltration Trenches Using Closed-Form Analytical Equations. Water Resources Management, 2020, 34, 3809-3821.	3.9	8
156	Effects of Relaxed Minimum Pipe Diameters on Fire Flow, Cost, and Water Quality Indicators in Drinking Water Distribution Networks. Journal of Water Resources Planning and Management - ASCE, 2020, 146, .	2.6	8
157	Single-Nucleus Chromatin Accessibility Landscape Reveals Diversity in Regulatory Regions Across Distinct Adult Rat Cortex. Frontiers in Molecular Neuroscience, 2021, 14, 651355.	2.9	8
158	Microwave Dielectric Properties of Ba6-3xSm8+2xTi18O54(x=2/3) Ceramics Produced by Spark Plasma Sintering. Japanese Journal of Applied Physics, 2003, 42, 7410-7413.	1.5	7
159	Highly piezoelectric lead-free ceramic powder: An efficient and eco-friendly multifunctional photocatalyst. Ceramics International, 2020, 46, 25266-25272.	4.8	7
160	Thermal plasma treatment of stormwater detention pond sludge. Pure and Applied Chemistry, 2008, 80, 1993-2002.	1.9	6
161	Size-controlled synthesis of BiFeO3 nanoparticles by a facile and stable sol–gel method. Journal of Materials Science: Materials in Electronics, 2016, 27, 10803-10809.	2.2	6
162	Effects of Demand, Mixing Fraction, and Rate Coefficient Uncertainty on Water Quality Models. Journal of Water Resources Planning and Management - ASCE, 2020, 146, .	2.6	6

#	Article	IF	CITATIONS
163	IMPROVEMENT OF ALKOXY-DERIVED HfO2 LAYERS FOR (Y, Yb)MnO3/HfO2/Si STRUCTURES. Integrated Ferroelectrics, 2006, 84, 121-127.	0.7	5
164	A three dimensional sulfur/reduced graphene oxide with embedded carbon nanotubes composite as a binder-free, free-standing cathode for lithium–sulfur batteries. RSC Advances, 2017, 7, 43483-43490.	3.6	5
165	A Tool for Water Balance Analysis of Bioretention Cells. Journal of Sustainable Water in the Built Environment, 2020, 6, .	1.6	5
166	Stochastic Rainwater Harvesting System Modeling Under Random Rainfall Features and Variable Water Demands. Water Resources Research, 2021, 57, e2021WR029731.	4.2	5
167	Discussion of "Analytical Solutions for Estimating Effective Discharge―by Peter Goodwin. Journal of Hydraulic Engineering, 2006, 132, 112-113.	1.5	4
168	Photovoltaic effect of TiO2 thick films with an ultrathin BiFeO3 as buffer layer. Applied Physics A: Materials Science and Processing, 2014, 117, 1301-1306.	2.3	4
169	Analysis of precipitation extremes in the Taihu Basin of China based on the regional L-moment method. Hydrology Research, 2017, 48, 468-479.	2.7	4
170	Tailoring the Piezoelectric and Photoluminescence Properties of Na0.5Bi0.5TiO3-K0.5Bi0.5TiO3-BaTiO3-Based Multifunctional Ceramics with Sm Doping. Journal of Electronic Materials, 2020, 49, 4923-4928.	2.2	4
171	Analytical derivation of urban flood frequency models accounting saturation-excess runoff generation. Journal of Hydrology, 2020, 584, 124713.	5.4	4
172	Seeking More Cost-Efficient Design Criteria for Infiltration Trenches. Journal of Sustainable Water in the Built Environment, 2021, 7, .	1.6	4
173	A cost-effective and solderability stretchable circuit boards for wearable devices. Sensors and Actuators A: Physical, 2021, 331, 112924.	4.1	4
174	CHEMICAL SOLUTION DEPOSITION AND ELECTRICAL PROPERTIES OF (100)-PREDOMINANT BaTiO3 THICKER FILMS. Integrated Ferroelectrics, 2007, 88, 51-57.	0.7	3
175	Bi4Ti3O12–(Ni0.5Zn0.5)Fe2O4 dielectric–ferromagnetic ceramic composites synthesized with nanopowders. Materials Chemistry and Physics, 2010, 124, 184-187.	4.0	3
176	Time course of the dependence of associative memory retrieval on the entorhinal cortex. Neurobiology of Learning and Memory, 2014, 116, 155-161.	1.9	3
177	Efficient induction of neural progenitor cells from human ESC/iPSCs on Type I Collagen. Science China Life Sciences, 2021, 64, 2100-2113.	4.9	3
178	Hypoproliferative human neural progenitor cell xenografts survived extendedly in the brain of immunocompetent rats. Stem Cell Research and Therapy, 2021, 12, 376.	5.5	3
179	Analytical Derivation of Urban Runoff-Volume Frequency Models. Journal of Sustainable Water in the Built Environment, 2022, 8, .	1.6	3
180	Analytical Equations for Direct Quantification of Green Roofs' Hydrologic Performance Statistics. Journal of Hydrologic Engineering - ASCE, 2022, 27, .	1.9	3

#	Article	IF	CITATIONS
181	Pulsed Arc Electrohydraulic Discharge characteristics and plasma parameters of sludge-water. , 2009, , .		2
182	Preparation and Dielectric Characteristics of Semitransparent CoFe2O4–P(VDF-TrFE) Nanocomposite Films. Journal of Electronic Materials, 2013, 42, 734-738.	2.2	1
183	Underestimation of flood quantiles from parallel drainage areas. Urban Water Journal, 2016, 13, 441-453.	2.1	1
184	Dielectric Properties of Alkoxy-Derived BaTiO <inf>3</inf> Films on LaNiO <inf>3</inf> /Pt/TiO <inf>x</inf> /Si(100). Applications of Ferroelectrics, IEEE International Symposium on, 2007, , .	0.0	0
185	Structural Disorder in the Key Lead-Free Piezoelectric Materials, and. Advances in Condensed Matter Physics, 2013, 2013, 1-5.	1.1	0
186	Discussion of "Green Infrastructure Recovery: Analysis of the Influence of Back-to-Back Rainfall Events―by Bridget M. Wadzuk, Conor Lewellyn, Ryan Lee, and Robert G. Traver. Journal of Sustainable Water in the Built Environment, 2018, 4, 07018001.	1.6	0